Research Article

Acute Effects of Passive Stretching on Skeletal Muscle Microvascular PO_2 and HIF-1α Expression: Influence of Stretch Intensity and Duration

Rin Kataoka[1)], Kazuki Hotta[1,2)], Yoshifumi Kurosaki[3)], Naohito Ishii[3)], Kota Izawa[1)], Narumi Fukuzaki[1)], Shuri Arai[1)], Kentaro Kamiya[1,2)], Judy Muller-Delp[4)], Atsuhiko Matsunaga[1,2)]

1) Department of Rehabilitation Sciences, Kitasato University Graduate School of Medical Sciences, Sagamihara, Japan

2) Department of Rehabilitation, School of Allied Health Sciences, Kitasato University, Sagamihara, Japan

3) Department of Medical Laboratory Sciences, School of Allied Health Sciences, Kitasato University, Sagamihara, Japan

4) Department of Anatomy and Physiology, Kansas State University, Manhattan, Kansas, United States

Short Title: Muscle stretch and microvascular PO_2

Corresponding Author

Kazuki Hotta, PT, Ph.D

Associate Professor

School of Allied Health Sciences, Kitasato University

1-15-1, Kitasato, Minami-ku, Sagamihara, Kanagawa, 252-0373, Japan

kazuki.hotta@gmail.com

TEL +81-42-778-9709

Keywords: muscle stretch, microvascular PO_2, hypoxia-inducible factor, phosphorescence quenching, microcirculation

NEW & NOTEWORTHY

The intramuscular oxygen dynamics during stretching remain unclear. Real-time changes in PO_2 during passive stretching were investigated using phosphorescence quenching. Microvascular PO_2 decreased in an intensity-dependent manner and remained low during prolonged stretching. The decline reached a plateau about 2 minutes after stretch onset. Moreover, 2 hours of sustained stretching downregulated HIF-1α mRNA. Collectively, these findings indicate that passive stretching induces acute, intensity-dependent microvascular hypoxia that persists and alters hypoxia-related transcriptional responses in skeletal muscle.

Abstract

This study investigated the acute effects of passive stretching on microvascular oxygen partial pressure ($PmvO_2$) and hypoxia-inducible factor-1α (HIF-1α) expression in rat skeletal muscle, focusing on stretch intensity and duration. Twenty male Wistar rats were assigned to either a stretch or sham group. In Study 1, the soleus muscle was passively stretched at varying intensities by changing its length from the optimal length (L_O) by 2, 4, 6, 8, and 10 mm, while $PmvO_2$ was simultaneously measured. In a separate experiment, the muscle was stretched from L_O to 8 mm and maintained in the stretched position for 2 hours, whereas in the sham group it was kept at L_O throughout. After stretching, the muscle was rapidly frozen, and HIF-1α mRNA was quantified by real-time PCR. Passive stretching induced an acute, intensity-dependent decrease in $PmvO_2$. Values during high-intensity stretches (6–10 mm) were significantly lower than in the sham group (25 ± 9 vs. 39 ± 7 mmHg, L_O vs. 8 mm; $P < 0.05$). Sustained 8 mm stretching caused a rapid decline in $PmvO_2$ within 40 s, followed by a stable low plateau for 2 hours (time $F = 11.2$; group $F = 17.9$; interaction $F = 2.10$; $P < 0.01$). Interestingly, 2 hours of stretching reduced HIF-1α mRNA expression. These findings demonstrate that passive stretching elicits an intensity-dependent and sustained reduction in microvascular PO_2, which may suppress HIF-1α mRNA expression in skeletal muscle.

Introduction

Passive stretching has been shown to induce long-term vascular and structural adaptations in skeletal muscle, including enhanced blood flow, improved endothelial function, and increased capillary density (1). These adaptive responses suggest that stretch generates early mechanotransductive and oxygen-related signals within muscle; however, the acute intramuscular oxygen dynamics that may trigger such adaptations remain unclear. Our previous work demonstrated that daily passive stretching using a dorsiflexion splint selectively elongates the soleus muscle and promotes marked microvascular adaptations (1). This finding suggests that soleus muscle is particularly responsive to stretch-related mechanical stimuli. Acute hemodynamic responses to muscle stretch has been also reported (2-4). Red blood cell (RBC) velocity and flux in intramuscular microvessels decrease progressively as muscle length increases (2). During the initial phase of muscle lengthening, microvessels become aligned more linearly along the muscle fiber axis, resulting in reduced tortuosity (3). Further increases in muscle length reduce microvessel diameter, increase vascular resistance, and thereby cause a decline in muscle blood flow by up to approximately 40% (4). These findings indicate that muscle stretch reduces RBC and oxygen delivery to the microvascular bed. However, the impact of muscle stretching on muscle PO_2 remains poorly understood. Although several human studies using near-infrared spectroscopy (NIRS) have shown reductions in tissue oxygenation during stretching (5-7), their findings are not entirely consistent. For example, while some studies report reductions in SmO_2 during stretching (5, 6), others — such as Brodeur et al. (7) — found no clear decrease. This variability may reflect differences in stretching protocols, including the target muscle, stretch intensity, duration, and whether the static was static or dynamic, passive or active. Thus, the acute intramuscular PO_2 responses to stretching remain incompletely understood. Because PO_2 represents the dynamic balance between oxygen delivery and oxygen consumption, direct in vivo measurement is essential to understanding how stretch perturbs intramuscular oxygen availability and potentially triggers downstream hypoxia-responsive signaling pathways.

In addition to altering muscle blood flow, stretching provides a mechanical stimulus to various cell types within the muscle. Mechanical stimulus such as stretch play a critical role in maintaining endothelial cell homeostasis (8). Endothelial cells can sense physical forces, including stretch and shear stress, and respond by altering gene expression, morphology, and function (9-11). Endothelial cells can sense not only mechanical stimuli but also chemical stimuli, such as oxygen, and trigger a variety of adaptive responses (12, 13). Muscle stretching is thought to promote adaptations in both muscle fibers (14) and endothelial cells (1, 15) through these mechanical and oxygen-related cues. However, the intramuscular oxygen dynamics during stretching and the subsequent expression of hypoxia-related genes remain unclear. Repeated stretch over several days or weeks has been shown to upregulate hypoxia-inducible factors (HIF-1α and HIF-2α) in skeletal muscle capillary endothelial cells (15), leading to increase expression of angiogenesis-related genes and enhanced microvascular density in skeletal muscle (1). These findings suggest that stretching promotes vascular remodeling in skeletal muscle via hypoxia-responsive signaling pathways (16). Nevertheless, it remains unclear how the magnitude and duration of stretch affect intramuscular PO_2 and whether such mechanical stimuli induce the expression of HIFs in skeletal muscle. We hypothesized that passive stretching reduces intramuscular microvascular oxygen partial pressure ($PmvO_2$), and that this reduction is dependent on the intensity of the stretch. The dependence on stretch intensity is presumed to result from the previously reported decrease in microvessel diameter (4, 17, 18). Furthermore, we hypothesized that exposure to localized hypoxia caused by stretching would induce the expression of HIF-1α mRNA in skeletal muscle. To test these hypotheses, the purpose of the present study was to investigate the acute effects of stretch on intramuscular $PmvO_2$ in rat skeletal muscle, with a specific focus on stretch intensity (Study 1) and duration (Study 2). Following the completion of PO_2 measurements, HIF-1α mRNA expression in the stretched and non-stretched muscle was quantified using real-time quantitative PCR (qPCR).

MATERIALS AND METHODS

Animals

Twenty male Wistar rats (10-13 weeks old; body weight 374±30 g; CLEA Japan, Tokyo) were used in the present study. The rats were maintained on a 12 h:12 h light-dark cycle and had free access to food and water. The animal experimental protocol was conducted in accordance with the Guiding Principles for the Care and Use of Animals in the Field of Physiological Sciences by the Japan Physiology Society, and approved by the Institutional Animal Care and Use Committee in Kitasato University School of Allied Health Sciences (Ei-ken 24-23-1). Of the 20 rats, 10 were used in study 1, 5 were used in study 2, and the remaining 5 served as a sham group for both Study 1 and 2.

Surgical preparation

Fig. 1 provides a schematic diagram illustrating the experimental setup. Rats were anesthetized with isoflurane (3% for induction, 1.5-1.8% for maintenance), concentration range known to minimize cardiovascular depression (19). Mean arterial pressure remained within a physiological range throughout the experiment, and the sham group served as an anesthetized control to account for any systemic effects of isoflurane. All surgical procedures were performed while monitoring rectal temperature, which was maintained at 37.0 °C using a heating pad (PhysioSuite, Kent Scientific, Torrington, CT, USA). A catheter was placed in the right common carotid artery and connected to blood pressure transducers (model MLT0670; ADInstruments Japan Inc.) and amplifiers (model FE117; ADInstru- ments Japan Inc.) to measure mean arterial pressure (MAP) and heart rate (HR). To perform stretching, the left soleus muscle was gently exposed without damaging the nerves or large blood vessels. The Achiles tendon connected to the soleus muscle was transected, and the distal end of the muscle was attached via a suture to a strain gauge (model MLTF500/ST; ADInstruments Japan Inc.)

mounted on a micromanipulator (Fig. 1). The micromanipulator was used to finely adjust the distance between the origin and insertion of the soleus muscle, thereby controlling the intensity of stretch. This setup enabled precise adjustment of muscle length in 1-mm increments. The exposed muscle tissue was continuously superfused with modified Krebs-Henseleit buffer (KHB: 132 mM NaCl, 4.7 mM KCI, 21.8 mM $NaHCO_3$, 2.0 mM $MgSO_4$, 2 mM $CaCl_2$-$2H_2O$) (20, 21). The KHB was adjusted to pH 7.4 at 37 °C using a brief application of 100% CO_2 gas (a few seconds) during preparation. The CO_2 exposure was used solely for fine pH adjustment and did not result in sustained hypercapnia or CO_2 equilibration of the solution. To prevent displacement of the proximal end of the soleus muscle during stretching, a suture was passed beneath the patellar tendon and secured on the side opposite to the strain gauge, as illustrated in Figure 1. This fixation ensured that both ends of the soleus muscle were immobilized. Subsequently, silver wire electrodes were sutured to the proximal and distal ends of the soleus muscle to determine its optimal length (L_O), which was later used as the baseline for stretch protocol. After completion of all experimental procedures, the rats were euthanized by heart extraction under 5% isoflurane anesthesia. The soleus muscles were carefully excised and weighed. In the sham group and the stretch group of Study 2, the mid-belly portion of the muscle was rapidly frozen, stored at −80 °C, and used for qPCR.

Muscle Stretching

Prior to applying stretch, a reference muscle length was defined. In this study, the muscle's optimal length (L_O) was designated as the baseline (0 mm). L_O is defined as the muscle length at which maximum active tension is generated (22). To determine the L_O, the soleus muscle was subjected to 7–10 tetanic contractions while incrementally adjusting muscle length. This procedure required approximately 1-2 minutes. Following the final tetanus, we waited at least 20 minutes before initiating baseline $PmvO_2$ recordings. During this period, both $PmvO_2$ and passive tension were confirmed to have returned to a stable baseline prior to starting the stretch protocols. Tetanic contractions were induced by electrical stimulation (100 Hz, 2 ms pulse duration, 1 s/3 s on/off 25% duty cycle; 80–100 V; Model SEN-2101, Nihon Kohden, Japan). Passive tension is defined as the force developed by a muscle during passive elongation in the absence of stimulation, primarily resulting from the elastic properties of structural components (23). In contrast, active tension is generated in reponse to electrical stimulation and arises from cross-bridge interactions between actin and myosin filaments within the muscle fibers (24). The tension measured by the strain gauge represents the sum of passive and active components. The tension recorded immediately before electrical stimulation was defined as passive tension. Accordingly, active tension was obtained by subtracting passive tension from the total tension during contraction (24). After setting the muscle length at the point where passive tension was 0 g, a single tetanic contraction was induced, and active tension was analyzed using LabChart (LabChart 8, ADInstruments Japan, Nagoya, Japan). The muscle was then stretched by 1-mm increments, and a tetanic contraction was repeatedly evoked at each length until the active tension reached its maximum value. The muscle length at which maximal active tension was obtained was defined as the L_O in this study.

Stretch Intensity Protocol (Study 1)

To examine the effect of stretch intensity on $PmvO_2$, ten male Wistar rats were used. The soleus muscle was incrementally stretched from its L_O, and $PmvO_2$ was recorded simultaneously. After maintaining the muscle at L_O (0 mm) for 3 minutes, the muscle length was sequentially adjusted for 3 minutes each to the following positions: 2, 0, 4, 0, 6, 0, 8, 0, 10, and 0 mm. Manual adjustments using a micromanipulator required approximately 1–3 seconds to transition between lengths. During each L_O phase, $PmvO_2$ and passive tension returned to stable baseline levels before the next stretch was initiated.

Stretch Duration Protocol (Study 2)

To evaluate the effect of stretch duration on $PmvO_2$, five male Wistar rats were used. The soleus muscle was maintained at a stretched position of 8 mm beyond its L_O for 120 minutes, while $PmvO_2$ was continuously recorded in real time throughout the experimental period. This stretch magnitude corresponded to the length at which a decrease in $PmvO_2$ was observed in the stretch intensity protocol. A 2-hour stretch duration was selected to characterize the full time course of intramuscular PO_2 during prolonged stretching. This duration allowed evaluation of not only the initial decline in $PmvO_2$ but also whether a stable plateau was maintained throughout sustained stretch. HIF-1α mRNA expression is reported to change within 24 hours after static stretch in skeletal muscle (15). Similarly, in human umbilical vein endothelial cells, hypoxia-induced changes in HIF-1α mRNA occur within 4 hours (25). The 2-hour duration was chosen to detect the hypoxia-induced changes and to characterize the full temporal profile of microvascular PO_2 during sustained stretching. Because the temporal kinetics of intramuscular PO_2 during sustained stretch were entirely unknown, a longer period was required to fully capture the onset, stabilization, and maintenance of PO_2 responses.

Sham procedure

In the sham group (n=5), the muscle length was maintained at the L_O throughout the 120 minutes, and $PmvO_2$ was measured over the same duration. To minimize the number of animals used, $PmvO_2$ data from the sham group were shared between studies 1 and 2. The inclusion of a sham group was necessary to account for potential changes in PO_2 resulting from the surgical exposure of skeletal muscle and prolonged observation under exposed conditions.

PO_2 measurement

Figure 1 illustrates the schematic diagram of $PmvO_2$ measurement using the phosphorescence quenching method. Measurements were performed with a phosphorometer (OxyLED, Oxyphor LCC, USA) and the phosphorescent probe Oxyphor PdG4 (Pd-meso-tetra-(3,5-dicarboxyphenyl)-tetrabenzoporphyrin; Oxyphor LLC, USA). Oxyphor PdG4 is a PEGylated dendrimer-based phosphorescent probe (molecular weight ~35 kDa) that remains confined to the vascular compartment due to its large hydrodynamic size. Previous studies have demonstrated that PdG4 shows minimal leakage from the vasculature for several hours and exhibits exceptional photostability during repeated excitation at frequencies up to 1–2 Hz (26). PdG4 even allows repeated oxygen imaging in the same animal on the following day, demonstrating its prolonged intravascular confinement (26). In this study, PdG4 was injected via the right carotid artery at a dose of 4 mg/kg of body weight (27), and $PmvO_2$ acquisition was initiated approximately 20 minutes later to ensure complete intravascular distribution of the probe. No baseline drift or signal deterioration was observed during the 2-hour recording period. The principles of the phosphorescence quenching technique have been described previously (26, 28), and detailed characterization of the Oxyphor PdG4 used in this study has been reported elsewhere (26). Briefly, this technique is based on the Stern–Volmer relationship, which quantitatively describes the oxygen dependence of the phosphorescent probe, and is expressed as follows:

$$PO_2 = \frac{(\tau_0/\tau) - 1}{kQ \times \tau_0}$$

where kQ is the quenching constant, and τ_0 and τ represent the phosphorescence lifetimes in the absence of O_2 and at a given PO_2, respectively. The phosphorescence lifetime (τ) is independent of the local probe concentration and is insensitive to the endogenous chromophores and fluorophores (29-31). A bifurcated light guide was positioned 2–5 mm above the surface of the exposed soleus muscle belly, and excitation light at 635 nm wavelength was applied. $PmvO_2$ was recorded every second in a dark room, allowing real-time monitoring PO_2 dynamics during stretching.

Curve fitting

To analyze the temporal dynamics of $PmvO_2$ in response to stretching (Study 2), nonlinear regression was performed using GraphPad Prism, version 10 (GraphPad Software). The fitting was applied over a 300-second interval, including 60 seconds of baseline at L_O and 240 seconds after the onset of stretch. For each rat (n = 5), the following equation was fitted:

$$\boldsymbol{PmvO}_{2(\boldsymbol{t})} = \begin{cases} \boldsymbol{Y_0}, & \boldsymbol{t} < \boldsymbol{X_0} \\ \boldsymbol{Plateau} + (\boldsymbol{Y_0} - \boldsymbol{Plateau}) \cdot \boldsymbol{e}^{-\boldsymbol{K}(\boldsymbol{t}-\boldsymbol{X_0})}, & \boldsymbol{t} \geq \boldsymbol{X_0} \end{cases}$$

Here, Y_0 represents the baseline $PmvO_2$ value, Plateau is the asymptotic value as time approaches infinity, K is the decay constant (with $\tau = 1/K$), and X_0 denotes the onset time of $PmvO_2$ decline. The adequacy of curve fitting was assessed based on the coefficient of determination (r^2), residual sum of squares (RSS), and visual inspection of residual plots. A threshold of $r^2 > 0.90$ was set for model acceptance. For each subject, the time required for $PmvO_2$ to reach within the 95% confidence interval (CI) of the plateau value was calculated, and the mean ± standard deviation across all animals was reported as the time required to reach a new steady state.

qPCR

Total RNA was extracted from frozen soleus muscle of rats using ISOGEN II (NIPPON GENE, Tokyo, Japan). The purity and concentration of the RNA were assessed by measuring the absorbance ratio at 260/280 nm using a NanoDrop Lite spectrophotometer (Thermo Fisher Scientific, Waltham, MA, USA). The extracted RNA was reverse-transcribed into cDNA using the PrimeScript RT-PCR Kit (Takara Bio, Shiga, Japan). Quantitative real-time PCR was performed using SYBR Green PCR Master Mix (NIPPON GENE, Tokyo, Japan) on a 7500 Real-Time PCR System (Applied Biosystems, Foster City, CA, USA) to measure the mRNA expression of HIF-1α (HIF1A), with β-actin (ACTB) used as the endogenous control. The primer sequences were as follows:

・HIF1A (HIF-1α):

Forward: 5′-TCAAGTCAGCAACGTGGAAG-3′

Reverse: 5′-TATCGAGGCTGTGTCGACTG-3′

・ACTB (β-actin):

Forward: 5′-ACGGTCAGGTCATCACTATCG-3′

Reverse: 5′-GGCATAGAGGTCTTTACGGATG-3′

Gene expression was analyzed using the delta-delta Ct method, and the results were normalized to the mean expression level of the sham group, which was set to 1.0.

Statical analysis

All statistical analyses were performed using GraphPad Prism version 10.0 (GraphPad Software). In the Study 1, to ensure signal stability, the average $PmvO_2$ value obtained the final 60 seconds of each 3 minutes period was used as the representative value for the stretch or L_O condition. In the Study 2, the baseline value was defined as the average $PmvO_2$ during the 1-minute period prior to stretch onset. For the first 4 minutes following the onset of stretch, representative values were calculated as the average for every 20-second interval. For the remaining duration, representative values were calculated every 15 minutes. Animal characteristics were compared between groups using one-way analysis of variance (ANOVA). Two-way repeated-measures ANOVA was used to analyze the effects of stretch length (Study 1) or time (Study 2) as the within-subject factor, and group (stretch vs. sham) as the between-subject factor. Tukey's post hoc test was applied for multiple comparisons when appropriate. All data are expressed as mean ± standard deviation, and statistical significance was defined as $p < 0.05$.

RESULTS

Animal chacteristics

There were no significant differences among the sham and stretch groups in body weight, heart weight, or soleus muscle weight (Table 1).

Study 1 (Stretch Intensity)

Passive stretching induced a progressive and intensity-dependent decrease in $PmvO_2$, which recovered upon return to the L_O (Fig 2). $PmvO_2$ was significantly lower in the stretch group than in the sham group under the 6, 8, and 10 mm stretch conditions (Fig 2; $p < 0.05$, respectively). In contrast, no significant differences were observed between groups during the recovery phases. A transient decrease in MAP was observed immediately in the stretch group at

6, 8, and 10 mm (Fig 3A; $p < 0.05$, respectively), whereas HR did not change significantly in eigher group (Fig 3B). In a supplemental post-hoc analysis, the MAP during each stretch phase was negatively correlated with stretch intensity (r_{rm} = –0.66, p = 0.001; Suppl Figure S1), indicating a strong negative correlation between stretch intensity and MAP.

Study 2 (Stretch Duration)

Prolonged passive stretching caused a rapid decrease in $PmvO_2$ that remained low throughout the 2-hour duration (Fig 4A). The first 300 seconds of $PmvO_2$ responses during the 2-hour stretch, along with the corresponding fitted curves, are presented in Supplemental Figure S2. Table 2 summarizes the result of the nonlinear regression analysis. Model fitting was good in all animals, with > 0.95 (Table 2). $PmvO_2$ reached a plateau within 121.8 ± 48.07 s after stretch onset (Table 2). A transient decrease in MAP occurred immediately after stretch onset but recovered thereafter (Fig 5A, 5C), while HR showed no persistent difference between groups (Fig 5B, 5D).

HIF-1α mRNA expression

Figure 6 shows the effect of 2-hour stretch on HIF-1α mRNA expression in the soleus muscle. HIF-1α mRNA expression was significantly lower in the stretch group compared to the sham group, which was maintained at L_O for 2 hours, as determined by qPCR (Fig 6; $p < 0.05$).

DISCUSSION

This study is the first to examine the effects of passive muscle stretching on microvascular oxygen dynamics in skeletal muscle. The principle findings were as follows: 1) $PmvO_2$ decreased during passive stretching; 2) the lower PmvO2 accompanied with the higher stretch intensity; 3) $PmvO_2$ rapidly declined after stretch onset, reached a plateau within approximately 2 minutes, and remained low throughout the 2-hour period; 4) HIF-1α mRNA expression in the soleus muscle was reduced by passive muscle stretching. Collectively, these results indicate that passive muscle stretching acutely and intensity-dependently decreases $PmvO_2$, sustains this reduction over time, and is associated with a concomitant suppression of HIF-1α mRNA expression.

In the present study, we clearly demonstrated that skeletal muscle $PmvO_2$ decreased in proportion to the intensity of passive stretch. $PmvO_2$ is considered to reflect the balance between oxygen delivery to capillaries and consumption (32). A previous human study that reported small increases (≈ 40 mL/min) in VO_2 during stretching used sit-and-reach–type movements that actually required voluntary effort, indicating that these protocols were not fully passive and elicited increases in HR (33). In contrast, the present experiments were conducted under anesthesia, producing a truly passive stretch without reflexive or voluntary muscle activation. Consistent with this, HR did not increase during stretching, suggesting that metabolic demand was minimally altered. Therefore, although a minor contribution from oxygen consumption cannot be entirely excluded, the predominant driver of the $PmvO_2$ reduction is likely reduced oxygen delivery rather than a meaningful increase in metabolic rate. Oxygen delivery to capillaries is influenced by several microcirculatory parameters, including capillary volume, functional surface area, RBC flux and velocity, hematocrit, and the path length and transit time of RBCs (32). Previous studies have shown that stretching reduces capillary tortuosity in skeletal muscle (4, 18, 34), leading to reductions in capillary diameter and blood flow (35, 36), as well as decreases in RBC velocity within capillaries (4). Furthermore, experiments conducted in anesthetized dogs demonstrated that passive stretch of respiratory muscles, including the diaphragm and parasternal intercostals, elevated intramuscular pressure and vascular resistance, resulting in transient occlusion or narrowing of arterioles, venules, and capillaries (37, 38). In the present study, at higher intensities of stretch (≥ 6 mm), a marked decrease in $PmvO_2$ was observed, which was presumably due to a reduction in RBC transport efficiency and consequently restricted oxygen delivery to the muscle. In the present study, muscle stretching was performed from the L_O. To estimate the sarcomere length corresponding to a 6-mm muscle extension, we referred to a previous study (34) showing that dorsiflexing the rat ankle from 90° to 60° lengthened the soleus muscle by 3–4 mm and increased sarcomere length from 2.55 µm to 3.17 µm ($\Delta \approx 0.62$ µm). Based on this relationship, the 6 mm stretch applied in the present study was estimated to increase sarcomere length to approximately 3.6–3.7 µm. This value exceeds the previously reported threshold range (3.2–3.4 µm), at which RBC velocity markedly decreases (4). These results suggested that increased vascular resistance likely contributed to the observed decrease in $PmvO_2$.

We also examined the temporal profile of $PmvO_2$ during the 2-hour stretching period. Because the temporal kinetics of $PmvO_2$ during sustained stretch had not previously been described, a 2-hour protocol was chosen to determine whether the stretch-induced reduction in oxygen availability was transient or maintained throughout the prolonged period. The time required for $PmvO_2$ to reach a plateau was approximately 122 seconds, indicating that a new steady state was established within about 2 minutes after stretch onset. This time course suggests that microvascular changes develop over the first few minutes following stretch initiation. In our previous clinical studies, passive stretching was typically maintained for only about 30 seconds (39, 40). However, the present findings newly demonstrate that it takes substantially longer for $PmvO_2$ to decrease and stabilize following stretch onset. In contrast, previous studies from our group showed that 30 minutes of static stretching using a dorsiflexion splint improved vascular endothelial function in older patients with peripheral artery disease (41) and in aged rats (1). The present findings indicate that such stretching protocols are sufficiently long to expose skeletal muscle to a hypoxic environment. Furthermore, we found that after the initial decline, $PmvO_2$ remained consistently low throughout the 2-hour stretching period. Because $PmvO_2$ reflects the balance between oxygen delivery and consumption in skeletal muscle (32), the sustained decrease observed in this study likely reflects a limitation in oxygen delivery due to increased vascular resistance. In addition to reduced oxygen delivery, the results also raise the possibility that oxygen consumption within the muscle increased during stretching. Endothelial cells are known to enhance oxygen utilization in response to mechanical stimulation (42). Although endothelial cells were not directly examined in the present study, previous reports have shown that mechanical stretch increases metabolic activity and oxygen consumption in endothelial cells. Piezo1 channels—which were not evaluated in the present study—are thought to mediate this response, as they are activated by mechanical stimuli such as stretch (43, 44). Activation of Piezo1 channels induces Ca^{2+} influx, which enhances mitochondrial respiration and subsequently promotes ATP production and oxygen utilization (42). These mechanisms may therefore contribute to the sustained oxygen consumption observed during stretching.

In addition, we observed a transient decrease in blood pressure during stretching. However, $PmvO_2$ continued to decline and remained low throughout the stretch period, even after blood pressure had recovered. Therefore, the reduction in $PmvO_2$ is unlikely to have resulted primarily from systemic hypotension. Rather, the sustained decline in $PmvO_2$ likely reflects local microvascular alterations, such as increased vascular resistance and reduced capillary perfusion. In contrast, previous studies have reported an increase in blood pressure during stretching (45). One of the major neural mechanisms regulating cardiovascular responses to muscle activity is the exercise pressor reflex, which is initiated by group III and IV muscle afferents in response to mechanical or metabolic stimuli (46). Passive stretching has also been shown to activate these afferents, leading to increased sympathetic excitation and a rise in arterial pressure (45).

Ishizawa et al. reported a stretch-induced pressor response in decerebrate, non-anesthetized rats (45). Methodological differences may explain this discrepancy, as the present experiments were performed under isoflurane anesthesia. It is possible that anesthesia transiently inhibited reflex pathways that normally elicit a pressor response during stretching. In previous work, including that of Ishizawa et al. (45), stretch was applied through calcaneal tendon traction, which simultaneously stretches the entire triceps surae muscle group. Because this muscle group is substantially larger than the soleus muscle alone, a greater number of mechanically sensitive group III–IV afferents would be expected to be activated, resulting in a stronger pressor response. In contrast, the present study selectively stretched the soleus muscle, and the smaller muscle mass may have resulted in less afferent recruitment, thereby limiting the magnitude of the stretch-induced pressor response.

In the present study, we investigated intramuscular oxygen dynamics and HIF-1α mRNA expression during the two hours of stretch. HIF-1α is a transcription factor that promotes the expression of angiogenesis-related genes under hypoxic conditions. Chronic passive stretching of skeletal muscle has been shown to induce localized hypoxia and upregulate HIF-1α and its downstream targets (1, 15, 47). However, most of these studies were conducted under chronic stretch conditions lasting several days to weeks, and little is known about the transcriptional regulation of HIF-1α during the acute phase. Unexpectedly, we observed a significant decrease in HIF-1α mRNA expression despite sustained low $PmvO_2$ conditions. This finding suggests that, during the early phase of stretch-induced hypoxia, mechanisms promoting HIF-1α mRNA destabilization may be preferentially activated. Although this regulatory mechanisms were not directly examined in the present study, previous reports have identified tristetraprolin and microRNA-429 as potential mediators of this process. Tristetraprolin binds to AU-rich elements within the 3′ untranslated region of HIF-1α mRNA and promote its degradation after prolonged hypoxic exposure (>3h) (48). In endothelial cells, microRNA-429 is transiently induced 2–4 hours after the onset of hypoxia and subsequently suppresses HIF-1α mRNA expression (49). Collectively, these observations support the idea that early stretch-induced hypoxia can activate pathways that destabilize HIF-1α mRNA. However, we cannot rule out additional contributions from non-hypoxic signals, including mechanical and inflammatory cues, which may also influence HIF-1α mRNA stability under the present experimental conditions.

Limitation

This study has several limitations. First, several key parameters-such as RBC flux, RBC velocity, hematocrit, and sarcomere length-were not directly measured. Consequently, the mechanisms underlying changes in $PmvO_2$ could not be fully elucidated. Future studies combining real-time measurements of these microcirculatory and structural parameters with $PmvO_2$ will provide a more comprehensive interpretation. Second, because the present study focused exclusively on the soleus, a predominantly type I muscle with known sensitivity to stretch-induced microvascular adaptations, the findings may not fully extend to muscles with different fiber-type compositions or architectural characteristics (1). In addition, stretch intensities in Study 1 were not randomized but applied in an ascending order. Although $PmvO_2$ and passive tension returned to baseline between stretches, future studies using randomized or counterbalanced protocols will be helpful to further exclude potential order effects. Finally, HIF-1α protein expression was not evaluated. Changes in mRNA expression do not always parallel protein levels, as previous studies have shown that HIF-1α protein can remain stable or even increase despite reduced HIF-1α mRNA expression (25, 48). To fully elucidate the acute hypoxic response to stretch, future research should examine HIF-1α/2α protein levels and downstream targets such as VEGF-A in parallel with mRNA levels. Because HIF-1α mRNA was quantified from whole-muscle homogenates, the observed decrease represents the net effect across multiple cell types within the muscle. Moreover, we did not assess inflammatory markers, so a contribution of stretch-induced inflammatory signaling (50, 51) to HIF-1α mRNA regulation cannot be excluded. Future studies combining cell-type-specific analyses (e.g., immunohistochemistry or in situ hybridization) with inflammatory readouts will be required to clarify how hypoxia-related and inflammatory pathways interact to regulate HIF signaling during passive stretch.

Summary and Conclusion.

Using real-time, in vivo phosphorescence quenching technique, this study demonstrated that passive stretching of rat skeletal muscle induces a stretch intensity-dependent decrease in $PmvO_2$, which is sustained throughout prolonged stretching. Furthermore, the sustained reduction in $PmvO_2$ was accompanied by suppressed HIF-1α mRNA expression, indicating that passive muscle stretch acutely modulates both intramuscular oxygen dynamics and the regulation of hypoxia-responsive gene expression.

GLOSSARY

$PmvO_2$: microvascular oxygen partial pressure

L_O: optimal muscle length

RBC: red blood cell

HIF-1α / HIF1A: hypoxia-inducible factor-1 alpha

HR: heart rate

MAP: mean arterial pressure

KHB: Krebs–Henseleit buffer

ACTB: β-actin

ANOVA: analysis of variance

CI: confidence interval

RSS: residual sum of squares

NIRS: near-infrared spectroscopy

qPCR: quantitative polymerase chain reaction

DATA AVAILABILITY

The datasets generated and/or analyzed in this study are available from the corresponding author on reasonable request.

ACKNOWLEDGMENTS

The authors are grateful to Ryota Miura for their excellent technical assistance.

GRANTS

This work was supported by JSPS KAKENHI Grant Number 24K14254.

DISCLOSURES

No conflicts of interest, financial or otherwise, are declared by the authors.

AUTHOR CONTRIBUTIONS

The experiments were conducted in the laboratories of the Department of Rehabilitation and the Department of Medical Laboratory Sciences, School of Allied Health Sciences, Kitasato University. R.K. and K.H. performed the data acquisition, analysis, and interpretation, and drafted the initial version of the manuscript. R.K., Y.K., and N.I. conducted the qPCR experiments. R.K., K.H., Y.K., N.I., K.I., N.F., S.A., K.K., J.M.-D., and A.M. contributed to the conception and design of the study and critically revised the manuscript for important intellectual content. All persons designated as authors qualify for authorship, and all those who are eligible for authorship are listed. All authors approved the final version of the manuscript and agreed to be accountable for all aspects of the work in ensuring that questions related to the accuracy or integrity of any part of the work are appropriately investigated and resolved.

SUPPLEMENTAL MATERIAL

Supplemental Fig. S1: DOI. 10.6084/m9.figshare.30733754

Supplemental Fig. S2: DOI. 10.6084/m9.figshare.30734066

FIGURE LEGENDS

Figure 1. Schematic diagram of the experimental setup for passive muscle stretching. Rats were anesthetized, and rectal temperature was continuously monitored and maintained at 37 °C using a heating pad. The left soleus muscle was surgically exposed and connected via a suture to a strain gauge and micromanipulator for precise control of muscle stretch in 1-mm increments. A catheter inserted into the right carotid artery was connected to a pressure transducer to monitor mean arterial pressure (MAP) and heart rate (HR). Microvascular oxygen partial pressure ($PmvO_2$) was measured during stretching using a phosphorometer positioned above the muscle in a dark room.

Figure 2. Changes in $PmvO_2$ with increasing stretch intensity The black and gray lines represent the mean values for the stretch group (n = 10) and the sham group (n = 5), respectively. Shaded areas indicate standard deviations. Stretch was applied stepwise from 2 to 10 mm, with the muscle returned to its optimal length (L_O) after each stretch. Each phase lasted 180 s, and the mean $PmvO_2$ during the final 60 s of each phase was used for analysis. Two-way ANOVA revealed a significant interaction between time and group ($F = 11.83$, $p < 0.001$) and a main effect of time ($F = 12.58$, $p < 0.001$), but not of group ($F = 0.64$, $p = 0.431$). $PmvO_2$ was significantly lower in the stretch group at 6, 8, and 10 mm compared with the sham group (* $p < 0.05$). $PmvO_2$: microvascular oxygen partial pressure; L_O: optimal muscle length.

Figure 3. Hemodynamic responses to increasing stretch intensity (A) Mean arterial pressure (MAP) and (B) heart rate (HR) during incremental stretch from 2 to 10 mm. Black and gray lines represent the mean values of the stretch group (n = 10) and the sham group (n = 5). Shaded areas indicate standard deviations. Stretch was applied stepwise, with the muscle returned to its optimal muscle length ($L_{O)}$ after each stretch. Each phase lasted 180 s, and the minimum value during each stretching phase was used for analysis. Two-way ANOVA showed a significant interaction between time and group in MAP ($F = 2.05$, $p = 0.031$). The minimum MAP at 10 mm was significantly lower in the stretch group (* $p < 0.05$). Two-way ANOVA using the minimum HR value from each phase revealed a significant main effect of time, whereas no significant main effect of interaction or group (Fig 3B; time $F = 4.26$, $p = 0.040$; interaction $F = 0.13$, $p = 0.998$; group $F = 0.24$, $p = 0.624$) was found. HR did not show a transient decrease in either group. MAP, mean arterial pressure; HR: heart rate; L_O: optimal muscle length.

Figure 4. Time course and early-phase dynamics of $PmvO_2$ during 120 minutes of stretch

(A) Mean $PmvO_2$ values in the stretch group (n = 5) and the sham group (n = 5). Black and gray lines represent group means, and shaded areas indicate standard deviations. Measurements included a 1-min baseline at the optimal muscle length (L_O) and 120 min following the onset of 8-mm stretch. Two-way ANOVA showed significant effects of time (F = 9.78, $p < 0.001$), group (F = 20.18, p =0.002), and their interaction (F = 8.97, $p < 0.001$). At baseline, there was no difference between groups. After the stretch onset, $PmvO_2$ declined rapidly in the stretch group and remained lower than in the sham group. The difference became significant within 20–40 s and persisted throughout the 120-min period (*$p < 0.05$). (B) Early-phase dynamics during the first 240 s after stretch onset. $PmvO_2$ showed a rapid decline followed by a plateau. Nonlinear regression demonstrated a good fit in all animals ($r^2 > 0.95$). On average, $PmvO_2$ reached the 95% confidence interval of the plateau within 121.8 ± 48.1 s. $PmvO_2$: microvascular oxygen partial pressure; L_O: optimal muscle length.

Figure 5. Hemodynamic responses to stretch duration

(A, C) Mean arterial pressure (MAP) and (B, D) heart rate (HR) during 120 min of sustained 8-mm stretch. Black and gray lines represent the mean values of the stretch group (n = 5) and the sham group (n = 5). Shaded areas indicate standard deviations. Measurements included a 1-min baseline at the optimal muscle length (L_O) followed by 120 min after stretch onset. MAP showed a significant interaction (Fig 5A, C; F = 2.33, p = 0.002) but no main effects. HR showed significant effects of interaction (F = 4.74, $p < 0.001$) and time (F = 7.09, $p < 0.001$) but not group (F = 0.47, p = 0.500). In the stretch group, MAP showed a transient decrease immediately after stretch but returned to levels comparable to those in the sham group (Fig 5C). HR changed significantly over time, but no persistent group difference was observed.

Figure 6. Effect of 120-minute stretch on HIF-1α mRNA expression

HIF-1α mRNA expression in the soleus muscle was assessed by quantitative PCR. The sham group (n = 5) was maintained at the optimal muscle length (L_O) for 120 min, whereas the stretch group (n = 5) underwent 120 min of sustained stretch. Expression levels were normalized to housekeeping gene (β-actin) and expressed relative to the sham mean. Data are presented as mean ± standard deviation. HIF-1α mRNA expression was significantly lower in the stretch group than in the sham group (* p = 0.002).

References

1. Hotta K, Behnke BJ, Arjmandi B, Ghosh P, Chen B, Brooks R, et al. Daily muscle stretching enhances blood flow, endothelial function, capillarity, vascular volume and connectivity in aged skeletal muscle. J Physiol. 2018;596(10):1903-17.
2. Kindig CA, Poole DC. Sarcomere length-induced alterations of capillary hemodynamics in rat spinotrapezius muscle: vasoactive vs passive control. Microvasc Res. 2001;61(1):64-74.
3. Mathieu-Costello O. Muscle capillary tortuosity in high altitude mice depends on sarcomere length. Respir Physiol. 1989;76(3):289-302.
4. Poole DC, Musch TI, Kindig CA. In vivo microvascular structural and functional consequences of muscle length changes. Am J Physiol. 1997;272(5 Pt 2):H2107-14.
5. Matsuo H, Kubota M, Shimada S, Kitade I, Matsumura M, Nonoyama T, et al. The Effect of Static Stretching Duration on Muscle Blood Volume and Oxygenation. J Strength Cond Res. 2022;36(2):379-85.
6. McCully KK. The influence of passive stretch on muscle oxygen saturation. Adv Exp Med Biol. 2010;662:317-22.
7. Brodeur ZR, Paustian MJ, Monteleone-Haught DA, Lamm RA, Pagano AG, Ellis CE. The Effects of Static and Dynamic Stretching on Muscle Oxygen Saturation in the Rectus Femoris. Int J Exerc Sci. 2022;15(3):702-8.
8. Jensen L, Bangsbo J, Hellsten Y. Effect of high intensity training on capillarization and presence of angiogenic factors in human skeletal muscle. J Physiol. 2004;557(Pt 2):571-82.
9. Naruse K, Yamada T, Sokabe M. Involvement of SA channels in orienting response of cultured endothelial cells to cyclic stretch. Am J Physiol. 1998;274(5):H1532-8.
10. Kuebler WM, Uhlig U, Goldmann T, Schael G, Kerem A, Exner K, et al. Stretch activates nitric oxide production in pulmonary vascular endothelial cells in situ. Am J Respir Crit Care Med. 2003;168(11):1391-8.
11. Thacher TN, Silacci P, Stergiopulos N, da Silva RF. Autonomous effects of shear stress and cyclic circumferential stretch regarding endothelial dysfunction and oxidative stress: an ex vivo arterial model. J Vasc Res. 2010;47(4):336-45.
12. Zhao M, Wang S, Zuo A, Zhang J, Wen W, Jiang W, et al. HIF-1alpha/JMJD1A signaling regulates inflammation and oxidative stress following hyperglycemia and hypoxia-induced vascular cell injury. Cell Mol Biol Lett. 2021;26(1):40.
13. Liu J, Wang W, Wang L, Chen S, Tian B, Huang K, et al. IL-33 Initiates Vascular Remodelling in Hypoxic Pulmonary Hypertension by up-Regulating HIF-1alpha and VEGF

Expression in Vascular Endothelial Cells. EBioMedicine. 2018;33:196-210.

14. Aoki MS, Miyabara EH, Soares AG, Saito ET, Moriscot AS. mTOR pathway inhibition attenuates skeletal muscle growth induced by stretching. Cell Tissue Res. 2006;324(1):149-56.

15. Milkiewicz M, Doyle JL, Fudalewski T, Ispanovic E, Aghasi M, Haas TL. HIF-1alpha and HIF-2alpha play a central role in stretch-induced but not shear-stress-induced angiogenesis in rat skeletal muscle. J Physiol. 2007;583(Pt 2):753-66.

16. Hotta K, Muller-Delp J. Microvascular Adaptations to Muscle Stretch: Findings From Animals and the Elderly. Front Physiol. 2022;13:939459.

17. Ellis CG, Mathieu-Costello O, Potter RF, MacDonald IC, Groom AC. Effect of sarcomere length on total capillary length in skeletal muscle: in vivo evidence for longitudinal stretching of capillaries. Microvasc Res. 1990;40(1):63-72.

18. Poole DC, Mathieu-Costello O. Skeletal muscle capillary geometry: adaptation to chronic hypoxia. Respir Physiol. 1989;77(1):21-9.

19. Wilding LA, Hampel JA, Khoury BM, Kang S, Machado-Aranda D, Raghavendran K, et al. Benefits of 21% Oxygen Compared with 100% Oxygen for Delivery of Isoflurane to Mice (Mus musculus) and Rats (Rattus norvegicus). J Am Assoc Lab Anim Sci. 2017;56(2):148-54.

20. Sonobe T, Inagaki T, Poole DC, Kano Y. Intracellular calcium accumulation following eccentric contractions in rat skeletal muscle in vivo: role of stretch-activated channels. Am J Physiol Regul Integr Comp Physiol. 2008;294(4):R1329-37.

21. Hotta K, Fujii Y, Hitosugi N, Takamizawa R, Inoue T, Tamiya H, et al. Effects of veno-arterial extracorporeal membrane oxygenation on skeletal muscle function and interstitial PO(2) in contracting muscle of normal rats. Microvasc Res. 2025;160:104813.

22. Holt NC, Azizi E. What drives activation-dependent shifts in the force-length curve? Biol Lett. 2014;10(9).

23. Sleboda DA, Wold ES, Roberts TJ. Passive muscle tension increases in proportion to intramuscular fluid volume. J Exp Biol. 2019;222(Pt 21).

24. Linke WA, Popov VI, Pollack GH. Passive and active tension in single cardiac myofibrils. Biophys J. 1994;67(2):782-92.

25. Jaskiewicz M, Moszynska A, Kroliczewski J, Cabaj A, Bartoszewska S, Charzynska A, et al. The transition from HIF-1 to HIF-2 during prolonged hypoxia results from reactivation of PHDs and HIF1A mRNA instability. Cell Mol Biol Lett. 2022;27(1):109.

26. Esipova TV, Karagodov A, Miller J, Wilson DF, Busch TM, Vinogradov SA. Two new "protected" oxyphors for biological oximetry: properties and application in tumor imaging. Anal Chem. 2011;83(22):8756-65.

27. Hirai DM, Craig JC, Colburn TD, Eshima H, Kano Y, Sexton WL, et al. Skeletal

muscle microvascular and interstitial PO2 from rest to contractions. J Physiol. 2018;596(5):869-83.

28. Behnke BJ, Kindig CA, Musch TI, Koga S, Poole DC. Dynamics of microvascular oxygen pressure across the rest-exercise transition in rat skeletal muscle. Respir Physiol. 2001;126(1):53-63.

29. Wilson DF, Lee WM, Makonnen S, Finikova O, Apreleva S, Vinogradov SA. Oxygen pressures in the interstitial space and their relationship to those in the blood plasma in resting skeletal muscle. J Appl Physiol (1985). 2006;101(6):1648-56.

30. Yu J, Ramadeen A, Tsui AK, Hu X, Zou L, Wilson DF, et al. Quantitative assessment of brain microvascular and tissue oxygenation during cardiac arrest and resuscitation in pigs. Anaesthesia. 2013;68(7):723-35.

31. Zhang C, Belanger S, Pouliot P, Lesage F. Measurement of Local Partial Pressure of Oxygen in the Brain Tissue under Normoxia and Epilepsy with Phosphorescence Lifetime Microscopy. PLoS One. 2015;10(8):e0135536.

32. Poole DC, Pittman RN, Musch TI, Ostergaard L. August Krogh's theory of muscle microvascular control and oxygen delivery: a paradigm shift based on new data. J Physiol. 2020;598(20):4473-507.

33. Arnold G. Nelson JK. Elevated metabolic rate during passive stretching is not a sufficient aerobic warm-up. J Sport Health Sci. 2013;2(2):109-14.

34. Ledvina MA, Segal SS. Sarcomere length and capillary curvature of rat hindlimb muscles in vivo. J Appl Physiol (1985). 1995;78(6):2047-51.

35. Welsh DG, Segal SS. Muscle length directs sympathetic nerve activity and vasomotor tone in resistance vessels of hamster retractor. Circ Res. 1996;79(3):551-9.

36. Supinski GS, Bark H, Guanciale A, Kelsen SG. Effect of alterations in muscle fiber length on diaphragm blood flow. J Appl Physiol (1985). 1986;60(5):1789-96.

37. Hussain SN, Magder S. Diaphragmatic intramuscular pressure in relation to tension, shortening, and blood flow. J Appl Physiol (1985). 1991;71(1):159-67.

38. Leenaerts P, Decramer M. Respiratory changes in parasternal intercostal intramuscular pressure. J Appl Physiol (1985). 1990;68(3):868-75.

39. Kato M, Masuda T, Ogano M, Hotta K, Takagi H, Tanaka S, et al. Stretching Exercises Improve Vascular Endothelial Dysfunction Through Attenuation of Oxidative Stress in Chronic Heart Failure Patients With an Implantable Cardioverter Defibrillator. J Cardiopulm Rehabil Prev. 2017;37(2):130-8.

40. Hotta K, Kamiya K, Shimizu R, Yokoyama M, Nakamura-Ogura M, Tabata M, et al. Stretching exercises enhance vascular endothelial function and improve peripheral circulation in patients with acute myocardial infarction. Int Heart J. 2013;54(2):59-63.

41. Hotta K, Batchelor WB, Graven J, Dahya V, Noel TE, Ghai A, et al. Daily Passive Muscle Stretching Improves Flow-Mediated Dilation of Popliteal Artery and 6-minute Walk Test in Elderly Patients with Stable Symptomatic Peripheral Artery Disease. Cardiovasc Revasc Med. 2019;20(8):642-8.
42. Jiang M, Zhang YX, Bu WJ, Li P, Chen JH, Cao M, et al. Piezo1 channel activation stimulates ATP production through enhancing mitochondrial respiration and glycolysis in vascular endothelial cells. Br J Pharmacol. 2023;180(14):1862-77.
43. Coste B, Xiao B, Santos JS, Syeda R, Grandl J, Spencer KS, et al. Piezo proteins are pore-forming subunits of mechanically activated channels. Nature. 2012;483(7388):176-81.
44. Li J, Hou B, Tumova S, Muraki K, Bruns A, Ludlow MJ, et al. Piezo1 integration of vascular architecture with physiological force. Nature. 2014;515(7526):279-82.
45. Ishizawa R, Estrada JA, Kim HK, Hotta N, Fukazawa A, Iwamoto GA, et al. Neural discharge of muscle afferents and pressor response to mechanical stimulation are associated with muscle deformation velocity in rats. Am J Physiol Regul Integr Comp Physiol. 2023;325(1):R13-R20.
46. Mitchell JH, Kaufman MP, Iwamoto GA. The exercise pressor reflex: its cardiovascular effects, afferent mechanisms, and central pathways. Annu Rev Physiol. 1983;45:229-42.
47. Milkiewicz M, Haas TL. Effect of mechanical stretch on HIF-1alpha and MMP-2 expression in capillaries isolated from overloaded skeletal muscles: laser capture microdissection study. Am J Physiol Heart Circ Physiol. 2005;289(3):H1315-20.
48. Chamboredon S, Ciais D, Desroches-Castan A, Savi P, Bono F, Feige JJ, et al. Hypoxia-inducible factor-1alpha mRNA: a new target for destabilization by tristetraprolin in endothelial cells. Mol Biol Cell. 2011;22(18):3366-78.
49. Bartoszewska S, Kochan K, Piotrowski A, Kamysz W, Ochocka RJ, Collawn JF, et al. The hypoxia-inducible miR-429 regulates hypoxia-inducible factor-1alpha expression in human endothelial cells through a negative feedback loop. FASEB J. 2015;29(4):1467-79.
50. Kamal KY, Othman MA, Kim JH, Lawler JM. Bioreactor development for skeletal muscle hypertrophy and atrophy by manipulating uniaxial cyclic strain: proof of concept. NPJ Microgravity. 2024;10(1):62.
51. Chen R, Feng L, Ruan M, Liu X, Adriouch S, Liao H. Mechanical-stretch of C2C12 myoblasts inhibits expression of Toll-like receptor 3 (TLR3) and of autoantigens associated with inflammatory myopathies. PLoS One. 2013;8(11):e79930.

Figure 1

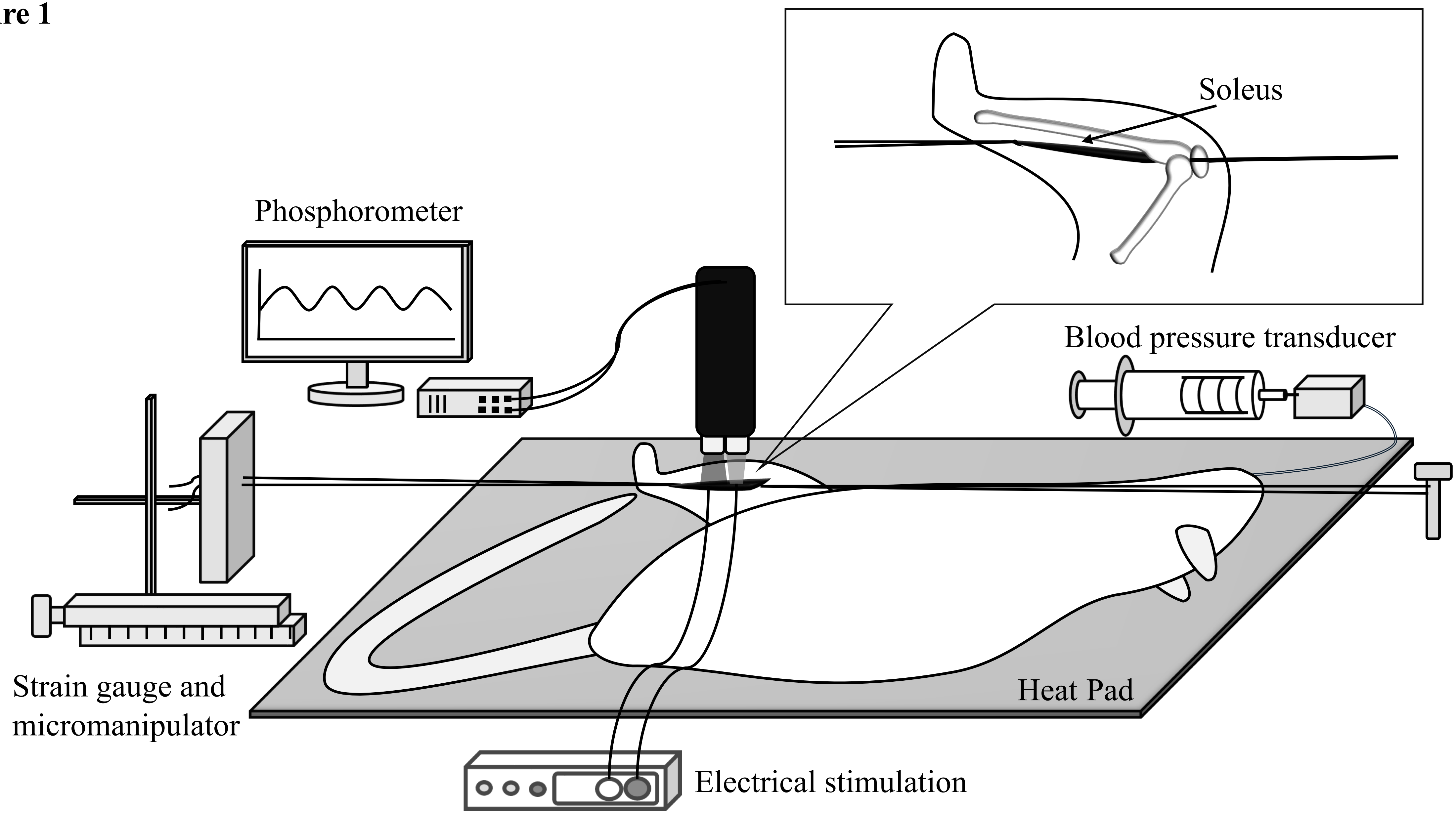
Soleus
Phosphorometer
Blood pressure transducer
Strain gauge and
micromanipulator
Heat Pad
Electrical stimulation

Figure 2

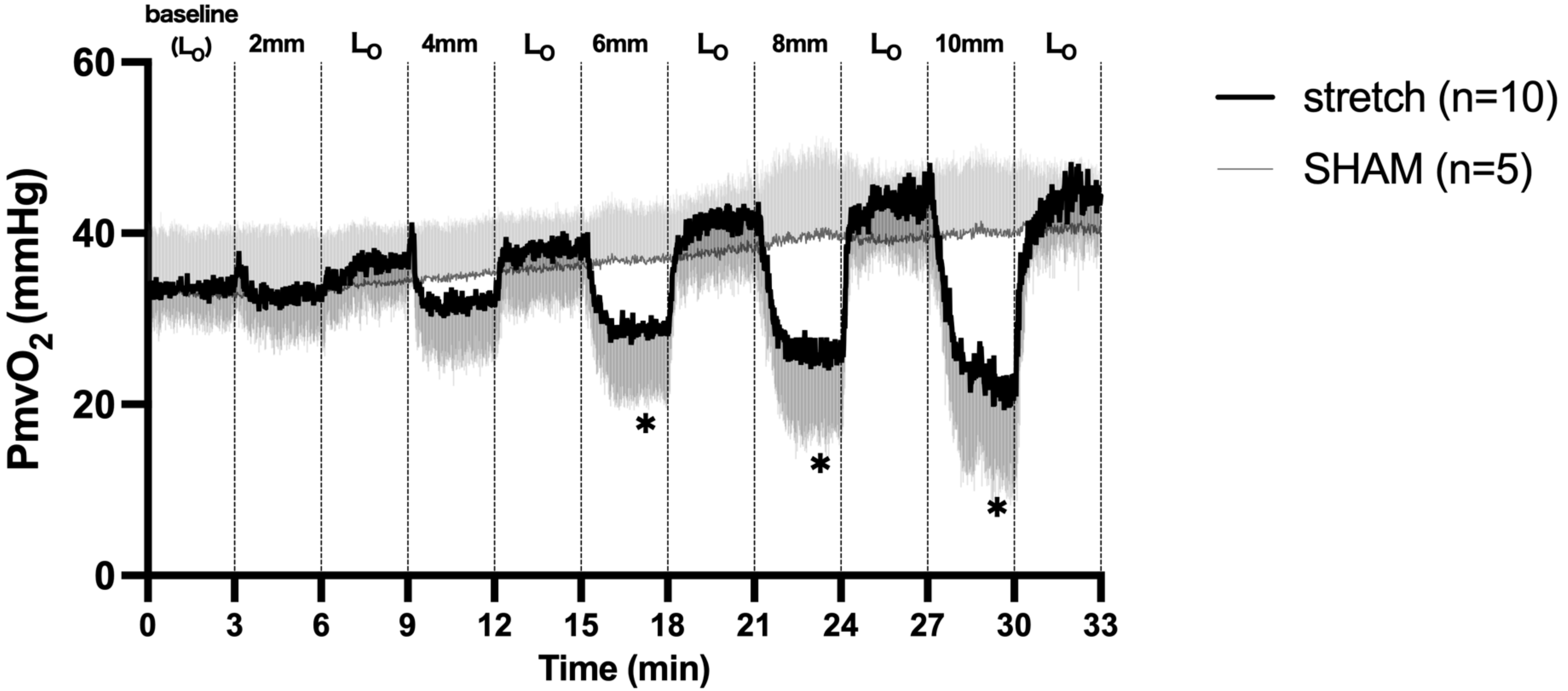

baseline
(Lo)
2mm
Lo
4mm
Lo
6mm
Lo
8mm
Lo
10mm
Lo
60
40
20
0
PmvO2 (mmHg)
0
3
6
9
12
15
18
21
24
27
30
33
Time (min)
*
*
*
stretch (n=10)
SHAM (n=5)

Figure 3

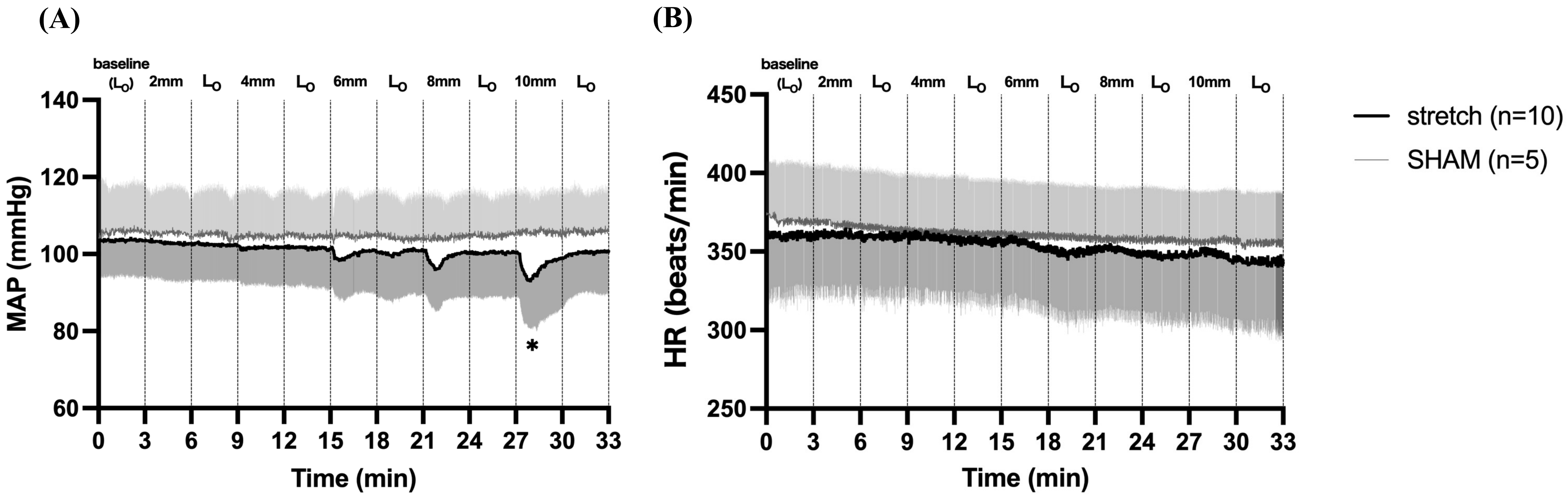
(A)
baseline
(Lo)
2mm
Lo
4mm
6mm
8mm
10mm
MAP (mmHg)
140
120
100
80
60
*
0
3
6
9
12
15
18
21
24
27
30
33
Time (min)
(B)
HR (beats/min)
450
400
350
300
250
stretch (n=10)
SHAM (n=5)

Figure 4

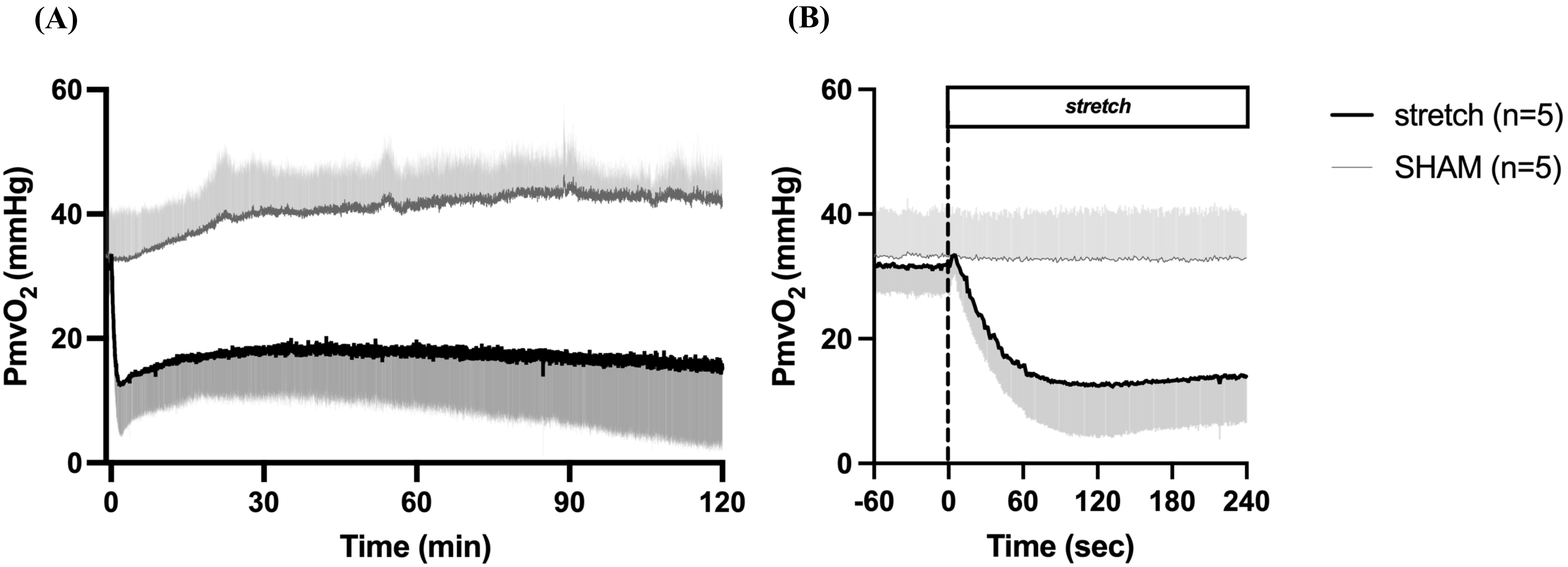
(A)
(B)
PmvO2 (mmHg)
60
40
20
0
0
30
60
90
120
Time (min)
stretch
-60
0
60
120
180
240
Time (sec)
stretch (n=5)
SHAM (n=5)

Figure 5

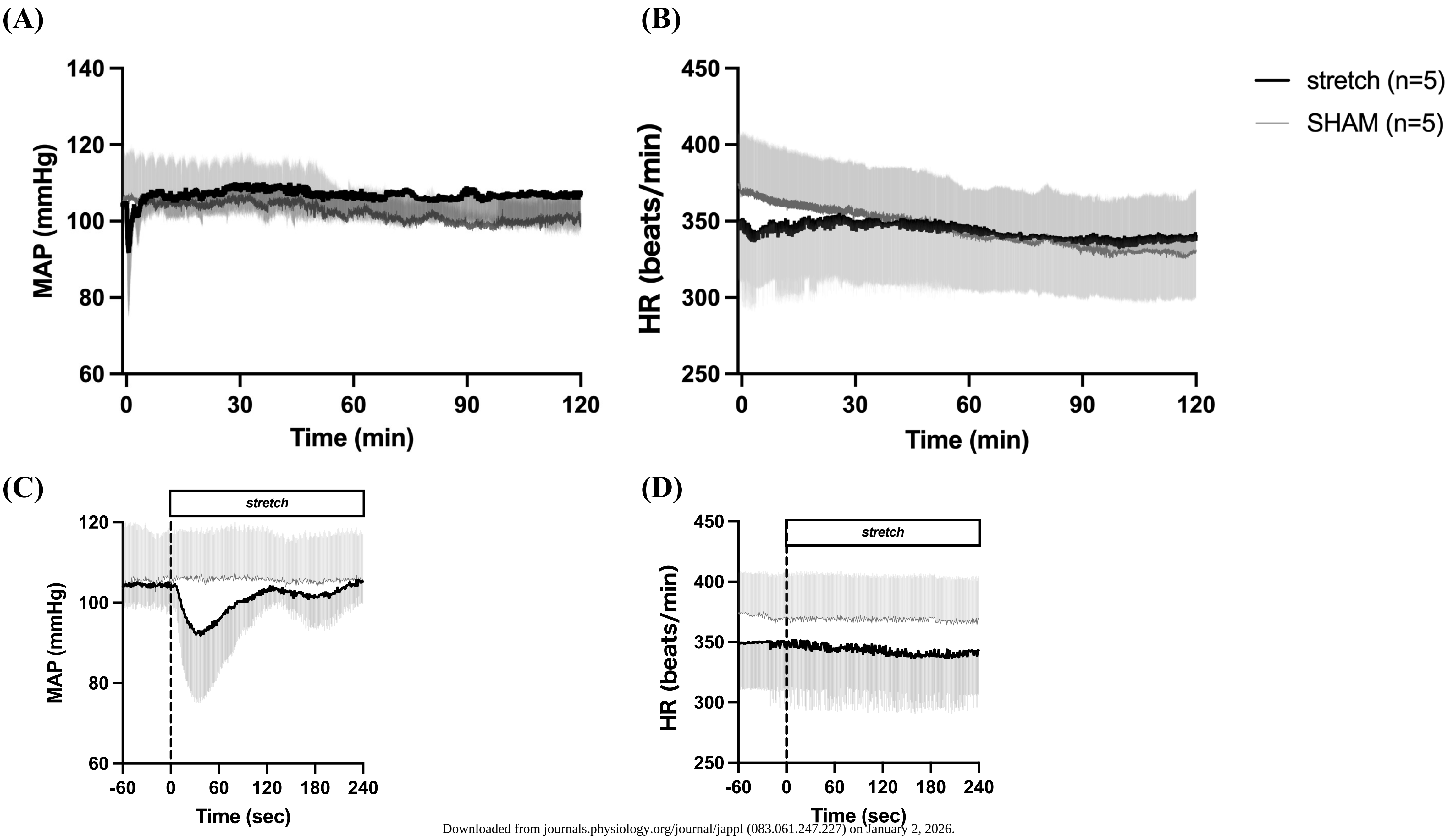
(A)
(B)
stretch (n=5)
SHAM (n=5)
MAP (mmHg)
140
120
100
80
60
0
30
60
90
120
Time (min)
HR (beats/min)
450
400
350
300
250
0
30
60
90
120
Time (min)
(C)
stretch
MAP (mmHg)
120
100
80
60
-60
0
60
120
180
240
Time (sec)
(D)
stretch
HR (beats/min)
450
400
350
300
250
-60
0
60
120
180
240
Time (sec)

Figure 6

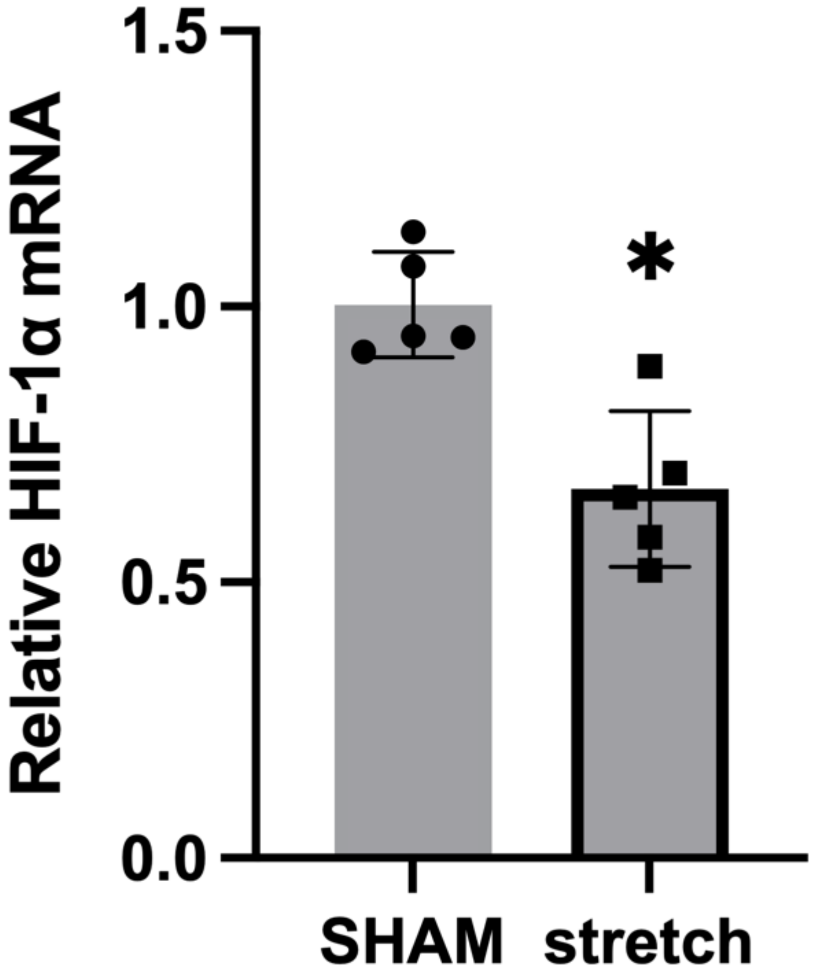

Table 1 Animal characteristics

	SHAM	stretch (study 1)	stretch (study 2)	
n	5	10	5	
Body Weight, g	367.8±20	370.4±30	386.2±36	F= 0.58 P= 0.56
Heart weight/body weight, mg/g	2.84±0.22	2.86±0.20	2.71±0.21	F=0.77 P= 0.47
Soleus muscle weight/body weight, mg/g	0.37±0.05	0.45±0.06	0.40±0.07	F=2.52 P=0.10

Values are means ± SD.

Table 2 Nonlinear Regression Analysis

Parameters	
X0	12.03 ± 3.08
Y0	31.75 ± 4.19
Plateau	13.27 ± 7.53
k	0.07 ± 0.06
Tau	21.31 ± 10.17
Values are means ± SD.	

Note: Data are presented as mean ± standard deviation (n = 5).

Abbreviations: PO_2, partial pressure of oxygen; τ, time constant; X0, onset time of $PmvO_2$ decline; Y0, baseline $PmvO_2$; Plateau, asymptotic $PmvO_2$ value.

Acute Effects of Passive Stretching on Skeletal Muscle Microvascular PO_2 and HIF-1α Expression : Influence of Stretch Intensity and Duration

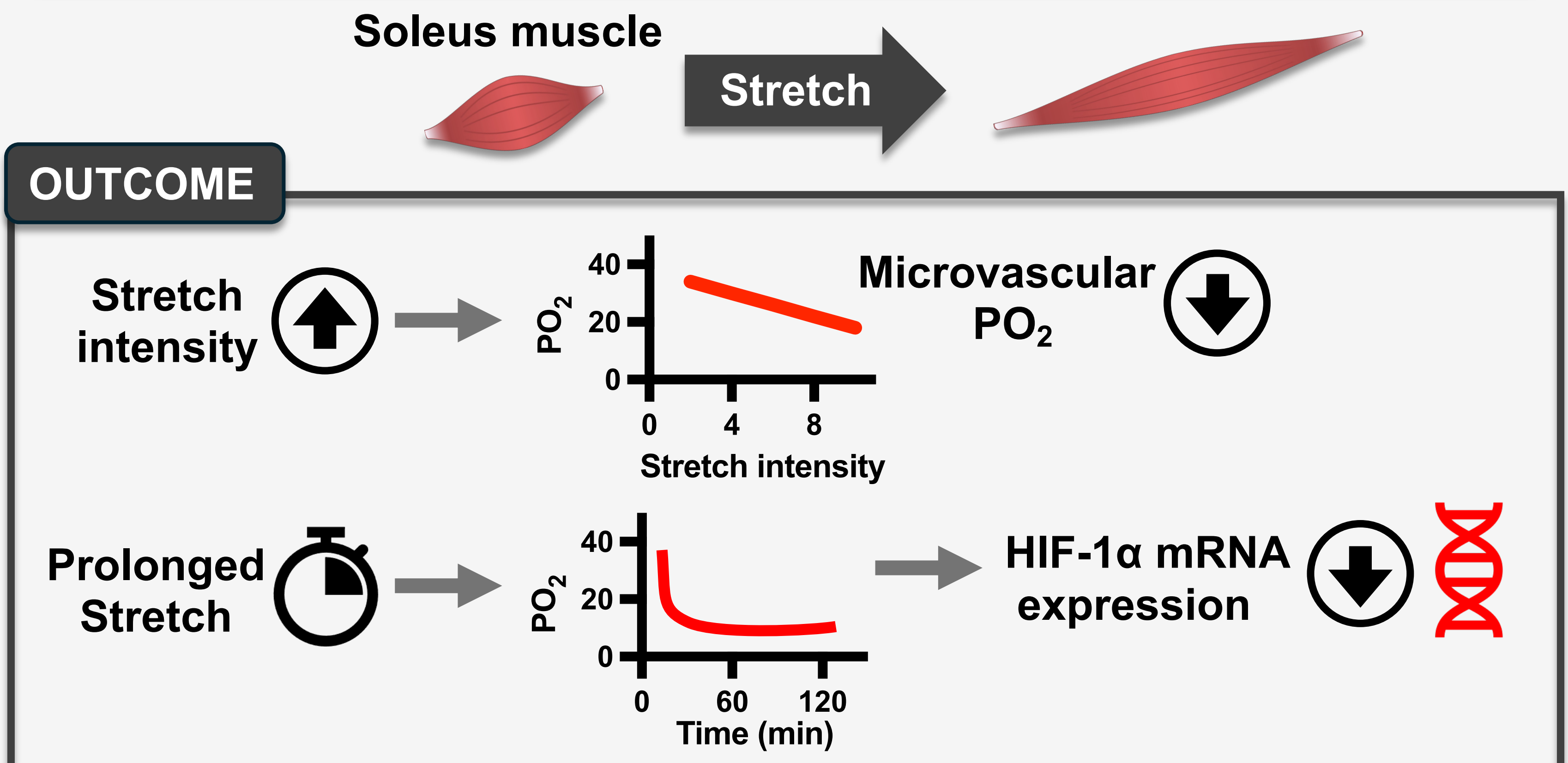

CONCLUSION

Passive muscle stretch induces a stretch intensity–dependent decrease in microvascular PO_2, which is sustained throughout prolonged stretching. Furthermore, this sustained reduction in microvascular PO_2 is accompanied by suppressed HIF-1α mRNA expression.